



AN ABSTRACT OF THE THESIS OF

Ledah Casburn for the degree of Master of Science in Computer Science  
presented on June 14, 2006.

Title: A Data-Driven Model of Pedestrian Movement

Abstract approved: \_\_\_\_\_

Ronald A. Metoyer

This thesis presents a model for simulating individual pedestrian motion based on empirical data. The model keeps track of a pedestrian's position, orientation, and body configuration and leverages motion capture data to generate plausible motion. Our model can automatically incorporate a pedestrian's physical limitations when making movement decisions, since it takes into account the current configuration of the character. Models can also be built for generating heterogeneous crowds by collecting motion capture data that includes children, the elderly, pedestrians in wheelchairs, and people on crutches. In this thesis, we present a 2D model for an able-bodied male and demonstrate the realism of our approach with a few small scale simulations and a larger crowd evacuation scenario. Furthermore, we compare the speed and density of pedestrians walking in single file to existing empirical results. The thesis concludes with a discussion of our model and offers suggestions for further research.

©Copyright by Ledah Casburn

June 14, 2006

All Rights Reserved

A Data-Driven Model of Pedestrian Movement

by

Ledah Casburn

A THESIS

submitted to

Oregon State University

in partial fulfillment of  
the requirements for the  
degree of

Master of Science

Presented June 14, 2006  
Commencement June 2007

Master of Science thesis of Ledah Casburn presented on June 14, 2006

APPROVED:

---

Major Professor, representing Computer Science

---

Director of the School of Electrical Engineering and Computer Science

---

Dean of the Graduate School

I understand that my thesis will become part of the permanent collection of Oregon State University libraries. My signature below authorizes release of my thesis to any reader upon request.

---

Ledah Casburn, Author

## ACKNOWLEDGMENTS

I grateful to all of my committee members, for their time, effort, and willingness to serve on my committee. I would like to thank my advisor, Dr. Ronald Metoyer, for his patience and guidance throughout this process. I am humbled that he and Dr. Eric Mortensen invited me to study at Oregon State University and very grateful for their support.

## TABLE OF CONTENTS

	<u>Page</u>
1 INTRODUCTION .....	1
2 RELATED WORK .....	5
3 MODEL .....	11
3.1 Motion Graphs and Mobility Map .....	14
3.2 Mobility Map Problems .....	18
3.3 Clustered Mobility Maps .....	19
3.4 Capability-Behavior Model .....	21
4 ANALYSIS .....	25
4.1 Qualitative Analysis .....	25
4.2 Quantitative Analysis .....	29
5 DISCUSSION AND FUTURE WORK .....	36
5.1 Discussion .....	36
5.2 Future Work .....	39
6 CONCLUSION .....	44
BIBLIOGRAPHY .....	45

## LIST OF FIGURES

Figure	Page
1.1 Impression of motion capture system. Highly reflective optical markers placed on subject are recorded by infrared cameras as he walks. . .	3
3.1 Our kinematic human model consists of 30 joints. . . . .	12
3.2 Pieces of existing motion sequences, for example, from a right turn, walk straight, and left turn sequence, can be combined to yield new sequences. The transitions between the sequences should be smooth so the new motion looks seamless and natural. . . . .	13
3.3 For the transition from pose $i$ to pose $j$ to look smooth in the new sequence, the differences between their joint angles, joint angle velocities, and root velocity should be small. . . . .	15
3.4 Illustration of the movement options from one single pose in the mobility map. Each pose reachable from the current pose in 45 frames is called a movement option. The final position and final orientation with respect to the current pose is stored along with the sequence of poses leading to it. . . . .	17
3.5 Illustration of the effect clustering has on movement options. . . . .	20
3.6 A cost function ranks each movement option from the clustered mobility map. The cost depends on the distance from the target and the deviation between the facing direction and the target direction. . . . .	22
3.7 Since each mobility point is 1.5 seconds from pedestrian A's current position, we measure $d$ as the distance between a mobility point and the predicted position of pedestrian B. We use this distance to determine the cost due to the proximity of nearby pedestrians. . . . .	23
4.1 Snapshots of the doorway experiment. Pedestrians must approach the first door, move through it, and exit through the second door. . .	26
4.2 Pedestrians were told to cycle through the narrow corridor. Groups of people were asked to walk at different speeds and filtered in gradually to try to replicate actual conditions and maintain an even initial flow. Since there are too many people trying to get through the corridor than it will allow congestion forms upstream of the bottleneck. Figure courtesy of Daamen <i>et al.</i> . . . . .	27



LIST OF FIGURES (Continued)

<u>Figure</u>		<u>Page</u>
4.3	Snapshots from hallway experiments showing pedestrians walking down narrow corridor. . . . .	27
4.4	Snapshots from a simulation of 746 pedestrians evacuating an auditorium and adjacent offices. Total egress time for this simulation was 5 minutes and 16 seconds. . . . .	28
4.5	Fundamental diagrams showing the relationships between density and speed, flow and speed, and density and flow. Figure courtesy of Daamen <i>et al.</i> . . . . .	31
4.6	Experimental setup for the measurement of the velocity and density relationship for movement in a single file line. . . . .	32

# A DATA-DRIVEN MODEL OF PEDESTRIAN MOVEMENT

## 1. INTRODUCTION

With the persistent threat of terrorist attack and natural disasters, the issue of public safety is of rising concern. How prepared are we in the event that a catastrophe strikes within our transportation facilities, sports arenas, and high-rise office buildings? How can we ensure the safety of their occupants? We can, for example, train building occupants to practice emergency plans and evacuation drills, and we can design new facilities with the goal of providing for the fast and efficient egress of diverse populations. Our goal is to create realistic and reliable models for how people move. If we do this we can open the door for creating accurate and efficient simulations of diverse populations that can be used in the analysis of building design and the training for evacuation.

We hypothesize that realistic models of pedestrian motion will be useful for architects in evaluating the design of new facilities. Helbing illustrated that changing the shape of a room and placing obstacles strategically in a space can improve the effectiveness of egress by easing congestion and increasing the flow of pedestrians [12]. We hypothesize that the more realistic the models of pedestrian motion, the more accurate the results of the simulation. Architects could use these models to evaluate the design of their buildings under emergency conditions. By using a simulation, architects could make modifications and evaluate the effect of the change on the rate of egress. These models will help architects gain confidence that their designs adequately provide for the rapid egress of diverse populations.

Not only will realistic models of pedestrian motion be useful in designing new buildings, we hypothesize they will be useful for training and studying aspects of evacuation. To track the spread of disease or a bioterrorist agent among people during an evacuation, we need accurate models of how people move. This could help emergency responders plan appropriately for worst case scenarios. Furthermore, emergency personnel could use these models to learn to better manage evacuations of large crowds of people. In addition, building occupants could immerse themselves in a training environment where they practice evacuations. A simulation may provide a less disruptive, more convenient, and cost effective way to practice evacuation and emergency response decisions. Participants could practice strategies and react to emergencies without fear of personal injury and without the expense of practical drills. This is of particular importance in cases, such as large high-rise office buildings, when a full evacuation would be difficult.

We argue that in order for these devices to be effective, the participants must be able to suspend their disbelief and become engaged in the simulations. The closer the simulation mimics real life, the more believable it will be. No matter how realistic the simulation environment is, unless the people are believable the simulation will not be believable. Therefore, we need to see realism in the motion of the individual pedestrians and realism in the composition of the crowds. A crowd is more realistic when it contains motion from pedestrians with various physical capabilities, such as individuals of all ages, people in wheelchairs, and those using crutches. As we observe people walking everyday, we develop an acute sense of what natural looking human motion is. The more realistic the motion of the individual pedestrians in our simulations, the easier it will be for participants to suspend their disbelief. Abnormal accelerations and unnatural direction changes stand out and interfere with suspension of disbelief. Similarly,

homogeneity stands out since we are used to seeing diverse walking styles. We argue that the best way to build accurate models of how people move is to observe real people walking and build models from these observations. We could then use these models to build simulations of heterogeneous crowds.

This thesis introduces a new model of pedestrian motion for use in 2D simulations that is based on motion capture data. Our first step in building a model from observations was to record 3D walking motions from human subjects with motion capture equipment (Figure 1.1). In the simulation we maintain a



FIGURE 1.1. Impression of motion capture system. Highly reflective optical markers placed on subject are recorded by infrared cameras as he walks.

notion of the pedestrian's current state. Current state can be described by a pedestrian's position, orientation, and body configuration or pose. Poses are based on a 3D kinematic model of a human subject and consist of joint angles for one frame of motion. The set of poses that a pedestrian can be in is consistent with the motion data we have collected. Similarly, the motion generated for our pedestrians by our model is consistent with the recorded motions. While our ultimate goal is to generate motion for 3D simulations, our initial efforts focus on 2D simulations.

At any point in the simulation, we say a pedestrian has the capability to reach a number of spatial points within some small time step. The variety of these reachable points is determined by the pedestrian's current state. To move forward in the simulation, the pedestrian must select one of these locations and begin to move there. Thus, we say the pedestrian's behavior is reflected in its particular choice of movement. Hence, we call our model the capability-behavior model of pedestrian motion.

The remainder of this thesis progresses as follows. In chapter 2 we discuss some of the related work in pedestrian simulation and computer animation. We present our capability-behavior model in more detail in chapter 3. We describe the algorithm for generating the set of possible spatial points given the pedestrian's current state and the process for selecting one of these points for movement. Chapter 4 presents qualitative and quantitative results for validation of our model. We demonstrate the realism of our approach through a few small scale and one large scale simulations. In the few small scale examples, we look for self-organization and emerging crowd phenomena. In the larger test, we demonstrate the feasibility of our current simulator to move pedestrians around in more complex environments. In the last experiment, we compare speed and density of pedestrians walking in a single file line to existing empirical data. Finally, we discuss some of the problems with this model and offer suggestions for future work in chapter 5.

## 2. RELATED WORK

Pedestrian simulations can be modeled at the macroscopic or microscopic levels. Microscopic simulations focus on the pedestrian at the individual level whereas macroscopic simulations focus on the pedestrians collectively. Macroscopic simulations focus on the aggregate characteristics of pedestrian flow rather than consider the influence direct interactions between pedestrians can have on collective behavior. Macroscopic simulations treat pedestrians as a type of fluid flow and use partial differential equations to model the movement of pedestrians through a space. One such example is Helbing's use of fluid dynamics to model pedestrian movement [10], others include [6, 14–16]. These simulations are generally fast and can process large numbers of people quickly. However, there is concern that pedestrians do not exactly behave like liquid and therefore may not be appropriate to use fluid and gas equations directly to model them. For example, pedestrians when walking do not generally utilize the full extent of the space but rather leave small gaps; if the gaps are ignored the resulting flow would be higher. In addition, there are some behaviors, such as the affect that a physical disability can have on mobility, that cannot be simulated in the macroscopic level and therefore may cause the results to be less accurate. It is for these reasons that our interest lies in microscopic simulations.

Microscopic simulations consider the movement of pedestrians at the individual level. They treat pedestrians as individuals and model the individual's behavior with the expectation that dynamic crowd behaviors will emerge from the interactions between individuals and the environment. Microscopic simulations can be more complex than macroscopic simulations and, as such, are generally better for smaller scale simulations. Many microscopic simulations already exist,

and one way to group them is to divide them into cellular automata models, behavioral force models, and agent-based models. For a more complete survey of these models see Helbing *et al.* [12].

In cellular automata models, the simulation space is divided into regularly spaced grid cells and pedestrians can move from one cell to a neighboring one. A small set of local rules, based on the occupancy of neighboring cells, govern the pedestrian's action for the next move [4]. These models are computationally simple and thus able to simulate large numbers of people quickly, however, the nature of the grid causes the motion of the pedestrians to be discrete. Unfortunately, the discrete motion undermines our goal of creating accurate human motion.

In contrast to cellular automata models, behavioral force models use a continuous space which allows for the creation of more accurate motion. Pedestrians are represented as point-masses and move through the environment pushed along by external forces. Their positions and velocities are updated according to Newton's laws of motion. Helbing argued that humans are so familiar with their environment that their behaviors and actions become fairly predictable and automatic and thus we can model human behavior using equations of motion [11]. A person who sees that a wall is in front of them will not usually hit it nor do people tend to collide with each other or walk close to someone they do not know. A pedestrian's increasing discomfort with these situations can be modeled with a repulsive force that will keep them away from other people and obstacles. Similarly, the pedestrian's desire to reach a goal will act as an attractive force pulling him toward his target.

These behavioral force models can reproduce many existing crowd phenomena when crowd densities are high, such as lane formation when pedestrians are moving in opposite directions and jamming at exits. However, a couple of

issues can make them difficult to use in some cases. First, pedestrians inside dense crowds can exhibit an unnatural “jitter” motion due to the repulsive forces that keep the pedestrians apart. The pedestrians keep moving because the forces pushing them away from other pedestrians are too strong. Second, our experience with this model is that there is no single set of parameters that works for every simulation environment. Instead, the parameters have to be carefully tuned to fit the scenario being modeled. Finally, it is unclear how we could model people in wheelchairs, crutches, and individuals with limited mobility using this approach. For example, a person walking with crutches or using a wheelchair cannot instantaneously shift sideways to avoid collisions with other pedestrians.

Agent-based models are generally more computationally expensive than behavioral force or cellular automata models, yet their ability to allow each pedestrian to have unique behaviors makes it much easier to model heterogeneous populations. We classify our capability-behavior model as an agent-based model. Antonini *et al.* present an agent-based model that closely resembles ours [1]. They use a discrete choice framework calibrated from recorded video sequences to model the movement of pedestrians. They describe a discretized region of space in front of the pedestrian as the set of possible next moves that can be made. These moves become the alternatives in the choice set. Then for each time step, a pedestrian must move to a selection from the alternatives in the choice set. Each option in the choice set is evaluated using a utility function. The utility function scores the options based on a set of attributes that describe the alternatives, for instance, how aligned is the option with direction to goal, and the set of socio-economic attributes that describe the pedestrian, including, his or her speed [1]. Antonini *et al.* interpret the speed of the pedestrian to be an alternative specific socio-economic attribute. There may be unknown or unmeasurable factors that



affect the pedestrian's movement choice; thus an error term is used in conjunction with the utility to build a probability for choosing an alternative. The pedestrian selects an alternative according to these probabilities and moves there. The best choices correspond to the alternatives with the highest probabilities and will be selected most frequently. However, this does not guarantee the best moves will always be chosen, which allows for some variability or randomness in the pedestrian movement.

Our approaches are similar in that we are both using human motion data to build our models and choosing a movement option from among a set of possible next moves. Since we are using motion capture data, we retain information about what pose a pedestrian is in and thus are able to maintain some notion of what their physical limitations are. For example, a pedestrian in a fast walking stride might not be able to turn as suddenly as another in a standing position. It is not clear how the discrete choice model with the current utility function will be able to account for such factors.

Imagine an animator has already recorded a person walking and another person jumping, and now would like to animate a character who walks up to an obstacle and jumps over it. Most commonly, an animator would have to record a person walking up to an obstacle and jumping over it to achieve a natural animation. As motion capture becomes more accessible we do see an increase in available data; nonetheless it is still expensive, and it would be convenient to be able to reuse existing motion for different purposes, rather than recording new sequences. This concept has motivated research in human motion generation. We would like to be able to utilize the previously existing motion sequences in generating the animation for our character's new motion without having it look unnatural.

Recent advances in computer animation research have led to graph-based algorithms for generating natural human motion [2, 18, 20, 21]. These approaches build graphs to encode the possible transitions between sequences of motion in a database. Steps are made to ensure that only the smoothest transitions are made between frames of motion to ensure that a path through the graph yields a new, natural looking motion sequence. Graph-based approaches can generate very realistic looking motion for animated characters that adhere to some constraint, such as following a given path or reaching key animation frames. However they typically do so at the expense of a global search. The graph is searched for an optimal path through the data that meets some constraint and returns a new smooth sequence of human motion. To generate motion for our characters from the recorded walking sequences, we based our work on these motion graph techniques. We would like to be able to run large scale simulations at interactive rates and are therefore unable to utilize a global search technique at run-time. For this reason, we further process the graph to produce a data structure similar to Srinivasan *et al.* that sacrifices memory space for speed [24].

Another important area of research in computer animation and simulation is level of detail generation. Levels of detail are commonly used to increase the efficiency, for example, of rendering an animation. As the model or object is moved farther from the viewer, the amount of detail used to render it is decreased. This way one can trade accuracy, by switching to a level with less detail, in order to gain efficiency and speed. Most closely related to our work is that of Brogan and Hodgins [5]. They model a physically simulated character's ability to move given its current state. Physical simulations are run offline to generate a set of possible movement options from some initial states. These options describe the character's capabilities and limitations. At run-time rather than incur the cost of

physically simulating the character, a motion is generated from the set of possible precomputed moves. In this respect, Brogan and Hodgins trade accuracy of the physical simulation to increase processing speed and scalability.

To decide the next move for a character given its current state, the algorithm of Brogan and Hodgins searches for the initial state that most closely resembles the character's current state and compares the resulting set of movement options. Each of the movement options are weighed against the characters goals, such as the desire to follow a given trajectory. The algorithm interpolates between the two options that are closest to meeting these goals to produce the motion for the character. We take a similar approach, but instead of using a physical simulation to generate the set of capabilities for a particular state, we use motion capture data.

### 3. MODEL

Our goal is to build a 2D motion model that encodes the capabilities of a walking human. In previous models, a pedestrian's choice of movement is dependent upon, for example, its current velocity, desired direction of travel, proximity to neighboring pedestrians, obstacles, and walls. These models can also account for physical characteristics of the pedestrians, such as weight and size, when making movement decisions. However, we believe there are other characteristics that can also effect a pedestrian's ability to move, such as a disability or its current state. It is unlikely for a pedestrian who, for example, is in the middle of a walking stride to be able to execute a quick turning maneuver, whereas, if he were standing still he might. These limitations should constrain the set of movements available to our simulated pedestrians.

To be able to account for a pedestrian's physical characteristics and state when making decisions, we build our model from real human motion data that has been recorded from motion capture technology. Motion capture technology records motion that can be played back later in much the same way that a tape player records sound.

We used a Vicon 612 3D optical motion capture system with 6 high speed infrared cameras to collect all of our motion data [27]. The cameras were placed around the perimeter of an area around the subject whose data we were collecting and faced toward the center of activity. We placed reflective markers, 5 mm in diameter, on the subject in strategic locations to record joint angles. Only the reflective markers are visible to the infrared cameras. As the subject walks around the capture region, the cameras record the images of the markers. The motions were captured at a rate of 60Hz. Figure 1.1 gives an impression of a typical motion

capture session. Once the recording is complete, the Vicon system reconstructs the 3D location for each marker for each frame of motion. This data is then cleaned and converted to joint angles, according to our kinematic model of the subject (Figure 3.1), using the Vicon Workstation and BodyBuilder Software.

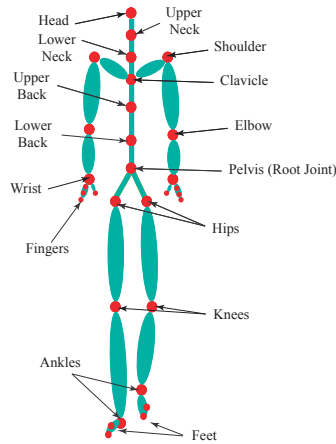


FIGURE 3.1. Our kinematic human model consists of 30 joints.

Our kinematic model is a hierarchical character that has 30 joints and whose root joint is centered at the pelvis. The position and orientation of the character is specified by the position and orientation of the root. The offset and orientation of each joint is specified with respect to its parent joint. For example, the location and orientation of the right knee is given with respect to the right hip joint. We define a pose to be the combination of the body's position and orientation at the root, and the set of angles for each joint for one frame of motion. Each joint has three degrees of rotational freedom corresponding to its Euler angles and thus contributes three floating point values. The root has six degrees of freedom to represent position and orientation of the body. Thus, for each frame, we have a total of 96 floating point values representing a pose.

We begin the process of building our model from observations by collecting 3D motion data from subjects using a Vicon optical motion capture system.

The subjects' motions were recorded as they performed various tasks relevant to pedestrian locomotion, such as walking straight at various rates, turning at various radii, coming to a stop, starting from a stop, and turning in place. For each subject, we took the recorded sequences of motion and combined the frames into a single database. To date, we have captured approximately 20 minutes of motion from a single individual, generating 114 sequences for a total of 33,404 poses in our database. We then use this database to build our motion model.

Motion capture can reproduce subtleties of human motion but we are restricted to motions that have already been captured and limited by the lack of control over our character's movements. Suppose we have recorded different motion sequences of a subject turning right, turning left, and walking straight, and now we would like to animate a pedestrian turning right around a corner, walking straight for a while, then turning left to cross a street. It would be convenient to be able to reuse this existing motion for animating our pedestrians (Figure 3.2). Therefore, we utilize existing motion generation techniques to construct new se-

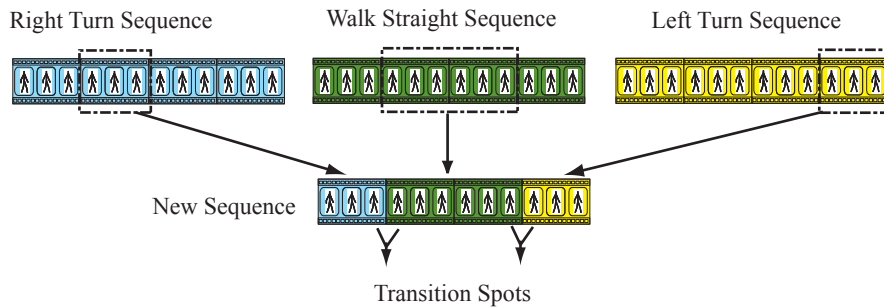


FIGURE 3.2. Pieces of existing motion sequences, for example, from a right turn, walk straight, and left turn sequence, can be combined to yield new sequences. The transitions between the sequences should be smooth so the new motion looks seamless and natural.

quences of motion for our animations without having the motion look unnatural [2, 18, 20, 21].

### 3.1. Motion Graphs and Mobility Map

Our 2D motion model is based on work from the 3D animation field in which motion capture data is used to generate the motion of 3D characters [2, 18, 20, 21]. Each of these techniques is based on the idea of using a graph. The frames are nodes, and the arcs represent possible transitions between the frames. More specifically, these motion graphs encode natural transitions between sequences of motion, for example, from poses that come from walking straight to those that come from turning. By traversing this graph we can generate new sequences of motion. Between any two poses in the graph, the path connecting them is a smooth sequence of poses that transitions the pedestrian from one pose to the other naturally. For example, the path connecting a pose in the middle of a walk cycle to a standing pose is a smooth sequence of motion that has the pedestrian finishing the walk cycle and coming to a stop.

Graph-based approaches typically perform a global search over the motion graph, looking for the smoothest sequence of poses that satisfies some constraint, such as finding the smoothest sequence that brings a pedestrian from its current location to a given spatial request. Research in this area has produced controllable characters whose motion also looks very real. The following section briefly explains the process of creating a motion graph. For more details about motion graphs, see [2, 18, 20, 21].

To build the motion graph we follow the same process as other researchers [2, 18, 20, 21]. We first build a fully connected graph. Its nodes are the poses

from our original motion sequences, and the arcs represent the cost to transition between poses. The transition cost function measures the similarity between any two poses  $i$  and  $j$  with respect to their joint angle differences,  $\Theta_{i,j}$ , joint velocities,  $\dot{\Theta}_{i,j}$ , and the linear velocity of the root,  $v_{i,j}$ . When the differences are small, the cost will be low. We use the same function to compute the transition cost as Srinivasan *et al.* It is calculated as follows:

$$\tau_{i,j} = \omega_{\Theta} * \Theta_{i,j} + \omega_{\dot{\Theta}} * \dot{\Theta}_{i,j} + \omega_v * v_{i,j}$$

where  $\omega_{\Theta}$ ,  $\omega_{\dot{\Theta}}$ , and  $\omega_v$  weight the joint angle, joint velocity, and root velocity differences respectively [24]. In general, the cost to transition from pose  $i$  in sequence 1 to pose  $j$  in sequence 2 is low if pose  $j$  is likely to follow pose  $i$  in a smooth motion sequence (Figure 3.3).

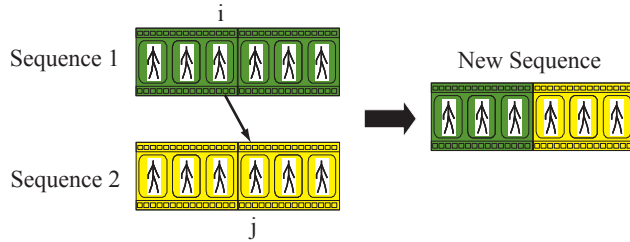


FIGURE 3.3. For the transition from pose  $i$  to pose  $j$  to look smooth in the new sequence, the differences between their joint angles, joint angle velocities, and root velocity should be small.

If the cost is too high, any transition between the poses may look unnatural and should not be considered. Therefore, we prune the graph to remove all transitions above a given threshold. Removing these transitions may introduce dead ends. Dead ends are nodes in the graph that have no outgoing transitions. If during motion generation we produced a sequence that included this dead end, the pedestrian would have no way to transition out of this pose and would be un-



able to continue moving. To ensure smooth and continuous playback these dead end nodes and nodes that lead only to dead ends must be removed. Ideally, any pose in the graph should be reachable from any other pose through some path. Therefore, we compute the largest strongly connected component and take that to be our motion graph. A walk through this graph produces smooth motion sequences between poses.

Rather than search the entire motion graph at run-time to animate our pedestrians, we take a similar approach to Srinivasan *et al.* to localize and limit the size of the search space in order to achieve interactive rates [24]. We try to precompute as much of the search as possible by using a data structure called a mobility map that sacrifices memory space for execution speed.

To build the mobility map we process the motion graph. For each pose in the graph, we compute the shortest path from it to every other pose in the graph. We call the result an “all pairs shortest path” (APSP) graph. The shortest path is defined as the sequence of poses that have the lowest cumulative transition cost. Since the transition cost is the lowest, following the shortest path between pairs of poses produces the smoothest and most natural motion sequence between them. For each pose in the APSP graph, we can identify a set of possible motions given this state. We collect all of the poses that can be reached in some time step, say 1.5 seconds or 45 frames. Then, for each of these reachable nodes, we store the sequence of poses along the path leading to the reachable node, and the relative change in position and orientation from the current node to the reachable node (Figure 3.4). The resulting data structure is what we call a mobility map.

During the simulation, pedestrians are animated by moving from one pose to another in a sequence. Pedestrians maintain information about which pose they are in, and at run-time they can use this pose to query the mobility map

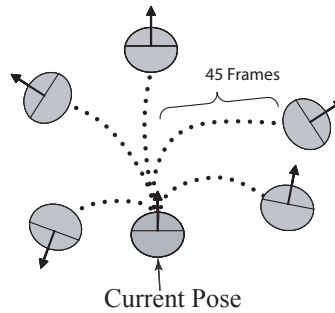


FIGURE 3.4. Illustration of the movement options from one single pose in the mobility map. Each pose reachable from the current pose in 45 frames is called a movement option. The final position and final orientation with respect to the current pose is stored along with the sequence of poses leading to it.

that is stored in memory. It returns the locations that can be reached in 1.5 seconds, how the pedestrian will be oriented, as well as the sequence of poses to get it there (Figure 3.4). These locations describe the pedestrian’s capabilities. The pedestrian is constrained to these movement options in deciding what their next move should be. Since a pedestrian’s motion at any time depends on its current state, two pedestrians may exhibit different behavior, even though they are using the same mobility map. From our observations, we found that the time step of 1.5 seconds is long enough to provide the pedestrian with a reasonable number of movement options, yet short enough to keep the memory requirements reasonable. It is important to note that the pedestrians can be interrupted at any point during the simulation to determine a new move, without having to finish motion playback from the previous move choice.

### 3.2. Mobility Map Problems

Using mobility maps, Srinivasan *et al.* have shown they can produce natural looking motion for 3D characters at interactive rates and have demonstrated the ability to maintain these rates for crowds of up to 500 pedestrians [24]. There remains, however, one limitation to this solution. Sometimes the smoothest sequence of poses may not yield the most direct path to a given spatial request. This lack of a direct path can cause the pedestrian to appear as though it is wandering. In most cases, there simply was not enough of the right kind of motion data in the database to be able to generate a smooth sequence from the pedestrian’s current location and pose to the desired location. Therefore, the character wanders until it reaches a more flexible area of the graph.

In 3D animations, the smoothness constraint is extremely important, as viewers, being accustomed to observing walking everyday, are very good at recognizing the subtleties of human walking motions. Even small discontinuities in the motion can become noticeable, which can undermine the viewer’s ability to suspend disbelief and become immersed in the training environment. Therefore, any synthesized motions used in our 3D animations must be smooth. Fortunately, we are not as attuned to the subtle differences in 2D motions and in our approach we can take advantage of the fact we are not creating 3D animations but developing 2D motion models. This allows us the freedom to relax the smoothness constraint and modify the mobility map approach in order to reduce the amount of wandering by keeping “more” of the data. As a result, we see an increase in the reactivity and controllability of the pedestrians.

In the next section we describe how similar poses can be grouped together into clusters, allowing us to build a more coarse-grained mobility map. The result

is a clustered mobility map, where each pose is replaced by a cluster of poses. The movement options of each pose in a cluster are combined to produce a larger number of movement options.

### 3.3. Clustered Mobility Maps

Within a time step of 1.5 seconds, a pedestrian has the capability to reach a number of spatial locations, which we call mobility points. The current body posture or pose that a pedestrian is in determines its mobility points and hence the type of motion it is capable of. For instance, if a pedestrian is standing in a pose with both feet on the floor, it is likely that he will continue to stand or begin to walk at a low velocity. In contrast, if the pedestrian has only one foot on the floor, the character may be in a position to move more quickly because it is likely in the middle of a walking stride. Likewise, the motions from similar poses should exhibit similar dynamics. For example, the motion sequences starting from one pose that has its left heel down and right toe pushing on the floor should share the same characteristics as motion sequences generated from another pose that also has its left heel down and right toe on the floor. It is possible that these poses generate different motion sets. One may generate motions that are right turns, whereas the other generates left turns, yet these motions should be possible from both poses. Therefore, we group similar poses together into a single cluster in order to generate a more complete set of options from the set of initial poses (Figure 3.5).

In order to identify groupings of similar poses, we use a subtractive clustering algorithm described by Kim *et al.* [17]. The algorithm estimates the number of clusters and their respective centers by first measuring the potential each pose

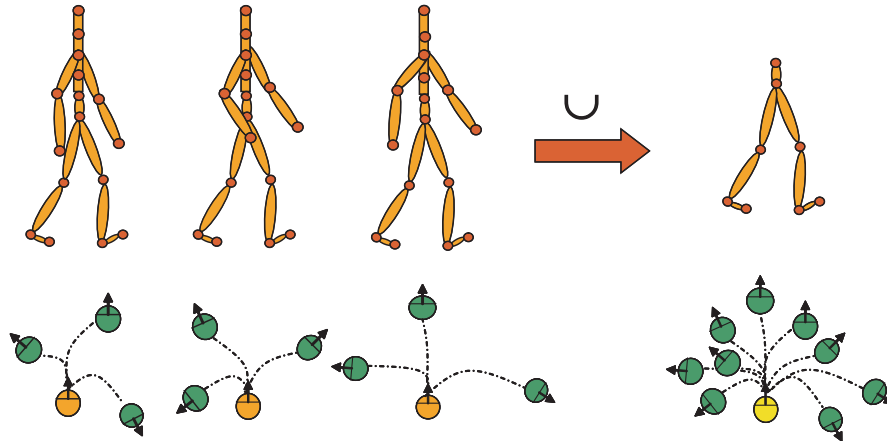


FIGURE 3.5. Illustration of the effect clustering has on movement options.

has for being a cluster center. The algorithm selects the pose with the highest potential to be a cluster center and then removes the effect of its potential from the rest of the poses. To determine the number of clusters, the algorithm iterates until the potential values for the remaining poses fall below a given threshold. To arrive at a threshold of 2.0, we experimented with a few values and visually examined the resulting clusters. The algorithm then compares the remaining poses against each cluster center and places them in the nearest cluster. In determining the clustering for an able-bodied pedestrian we can ignore the upper body. Therefore, to compare how close a pose is to a particular cluster center, we use nearly the same pose distance metric that we used in building the motion graph except that we set the upper body weights to zero.

The subtractive clustering algorithm generated a total of 670 clusters. The average number of poses in each cluster is approximately 50 with a standard deviation of 53 poses. Approximately 6.1% of the clusters contain more than 100 poses, with an average of 193 poses. The remaining clusters on average have only

40.5 poses. The clusters with the largest number of poses are comprised mainly of poses with two feet planted side by side.

Once the poses have been clustered, we can combine the individual mobility maps for each pose in a cluster into a single mobility map for the cluster. The cluster shares the movement options from all the poses within it, thus giving a simulated pedestrian more mobility and greater ability to react to movement requests. In related work, Srinivasan and Metoyer developed a metric for comparing the responsiveness of an animated character. In their experiments, they found that the pedestrians using this new clustered mobility map were quicker to respond to changes in movement requests and thus more controllable than the pedestrians using the unclustered mobility maps [25]. The following section describes how we use this new clustered mobility map to drive the 2D simulation.

### 3.4. Capability-Behavior Model

At run-time we use the clustered mobility map to generate the motion of each 2D pedestrian. At any point in time, a pedestrian will be in a particular pose of a cluster and will have movement options dictated by the mobility map of that cluster. We assume that the pedestrian simulator makes target requests for each pedestrian. We define a target as a position a pedestrian wants to reach, such as the location of the nearest exit. Pedestrians choose one of the options and the recorded motion is played to move them forward in time. Pedestrians move toward the targets to exit the building.

Given a target request, the movement options are first ranked based on a cost function:

$$C_i = \omega_D D + \omega_\theta \Theta - \omega_S S + \sum \omega_P P$$

The cost function is similar to Srinivasan *et al.* [24], where  $D$  measures the Euclidean distance from the mobility point to the target and  $\Theta$  is the deviation angle (Figure 3.6). The deviation angle is the angle between the facing direction a pedestrian has upon taking a movement option and the vector from the mobility point to the target. We modify the function to include a term,  $S$ , which encourages faster movement, and another term,  $P$ , which incorporates interference from neighboring pedestrians. The term,  $S$ , represents the distance from the pedestrian's current position to the mobility point. Options that move the pedestrian farther in 1.5 seconds will have a lower cost.

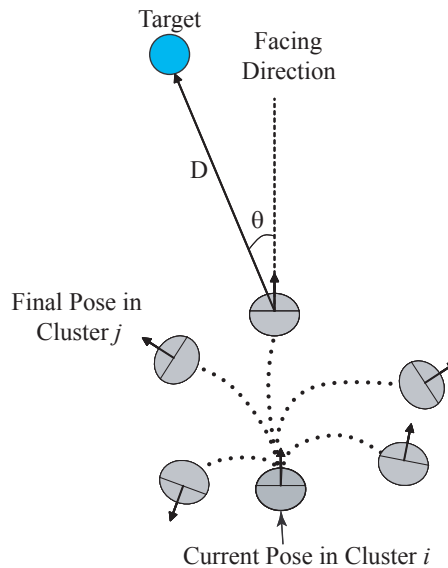


FIGURE 3.6. A cost function ranks each movement option from the clustered mobility map. The cost depends on the distance from the target and the deviation between the facing direction and the target direction.

The last term in the cost function measures the influence that proximity to neighboring pedestrians has on the choice of movement options. We represent this influence with a function similar to that used by Helbing and Molnar in the social forces model [11]. The closer the mobility point is to another pedestrian,

the higher the cost. If, however, the pedestrian is moving at a slower velocity, it will be more comfortable selecting a move that is close to another pedestrian. We represent the cost with a decreasing exponential function:

$$P = a * e^{-d/(b*v)}$$

where  $d$  is the distance between the pedestrian at the mobility point and the predicted position of another pedestrian (Figure 3.7). To compute the predicted position of the other pedestrians, we assume constant velocity over the time step. The velocity of the pedestrian at the mobility point is represented by  $v$ , while  $a$  and  $b$  are constants with values 10.5 and 0.09, respectively. These values were found through visual experimentation and used throughout all of our experiments. The total pedestrian interference for each movement option is the summation of the influences from each of the neighboring pedestrians. We use a grid subdivision scheme to determine the nearby pedestrians efficiently.

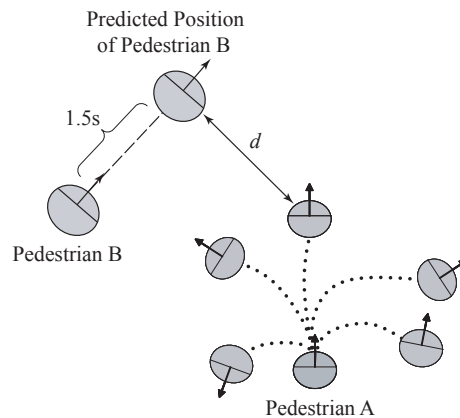


FIGURE 3.7. Since each mobility point is 1.5 seconds from pedestrian A's current position, we measure  $d$  as the distance between a mobility point and the predicted position of pedestrian B. We use this distance to determine the cost due to the proximity of nearby pedestrians.



Variables  $\omega_D$ ,  $\omega_\theta$ ,  $\omega_S$ , and  $\omega_P$  are weighting terms for the distance, deviation angle, speed, and pedestrian influence, respectively. Pedestrians that are behind the mobility point are not considered to be interfering. In this situation,  $\omega_P = 0$ , otherwise  $\omega_P = 1$ . We find the values 1.0, 2.5, and 0.4 work well for the weights  $\omega_D$ ,  $\omega_\theta$ , and  $\omega_S$  respectively.

We rank the movement options according to their cost and store them in a priority queue. The first option in the priority queue has the least cost. Our algorithm iteratively extracts the options from the queue and tests them for intersections with walls or nearby obstacles. We implemented a quadtree subdivision scheme to efficiently determine nearby obstacles and walls for intersection tests [9]. The first option with no intersections is chosen as the desired option; it is used to animate the motion of the pedestrian for the next 1.5 seconds or 45 frames. The pedestrian can be interrupted at anytime during the playback of the motion to plan its next move. Then from its current pose it will reevaluate its options from the corresponding cluster and choose another one. If the algorithm cannot find a suitable option, i.e. picking any option would cause the pedestrian to intersect an obstacle or wall, then we allow our pedestrian to linearly interpolate its position and orientation, for four frames, toward the goal. This allows the pedestrian to move into a position or face away from the obstacle so that at least one movement option can become feasible. In our experiments, the simulated pedestrians resort to the interpolation only 2% of the time.

In conclusion, the cost function leads the simulation to prefer movement options that quickly move the pedestrian closer to its target, orient the pedestrian toward the target, and keep the pedestrian away from its neighbors.

## 4. ANALYSIS

One of our goals is to create realistic and accurate models of how people move. In our previous chapter, we presented our prescribed motion model and illustrated how it could be used in our simulator. In this chapter we will present qualitative and quantitative results for validation of our model.

### 4.1. Qualitative Analysis

We demonstrate the realism of our approach through a few small scale simulations and one large scale simulation. In the small scale simulations, we look for self-organization of the individual pedestrians and emerging crowd phenomena, such as the formation of pedestrians into a zipper-like pattern in narrow spaces and crowding at doorways. In the larger scale simulation, we investigate the ability of our current simulator to move pedestrians around in more complex environments.

In all of our experiments, the pedestrians are represented by small black circles having diameter 0.4 meters; their velocity and facing direction is visualized by a light gray line projecting from the center of the circle (Figures 4.1, 4.3, and 4.4). In addition, all of the parameters of our capability-behavior model are identical and remain unchanged from experiment to experiment. No parameter tuning was necessary to make the capability-behavior model fit the particular situation being tested.

Our first small scale simulation illustrates the movement of pedestrians through a doorway (Figure 4.1). We populated a room 20.0 meters long and 10.0 meters wide with 50 pedestrians and watched their behavior as they exited through a door 1 meter wide. The pedestrians must exit the room through the first door, proceed forward through the next room and exit the building through

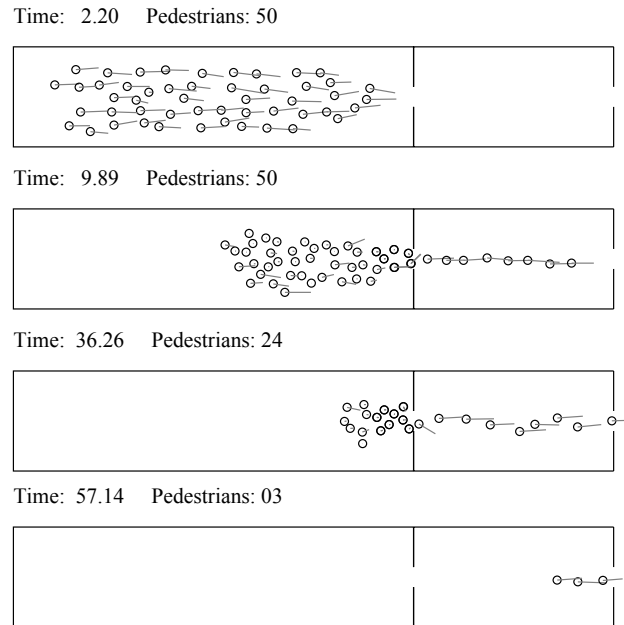


FIGURE 4.1. Snapshots of the doorway experiment. Pedestrians must approach the first door, move through it, and exit through the second door.

the second door. As the pedestrians move, they spread out and avoid collisions when there is enough space and bunch up when there is not. As the pedestrians try to move through the first door, the demand for egress becomes higher than the door can allow. We call the door a bottleneck since it restricts the flow of pedestrians through it. Congestion forms upstream of the bottleneck as the crowd of pedestrians stand and wait for their turn to pass through the door. We do not see any of the characteristic “jittering” of the pedestrians when they are close to each other that we see in the social forces model.

Daamen *et al.* have performed many experiments to try and learn the walking behavior of pedestrians. In one particular experiment, they studied the flow of pedestrians in bottlenecks [8]. They observed pedestrians walking from an open region, through a narrow corridor, and circling back around again. Figure

4.2 gives an impression of Daamen *et al.*'s experiment. From our observations, we find the shape of the congestion appearing before the bottleneck in our experiment (Figure 4.1) agrees with their empirical results (Figure 4.2).



FIGURE 4.2. Pedestrians were told to cycle through the narrow corridor. Groups of people were asked to walk at different speeds and filtered in gradually to try to replicate actual conditions and maintain an even initial flow. Since there are too many people trying to get through the corridor than it will allow congestion forms upstream of the bottleneck. Figure courtesy of Daamen *et al.*

In our next experiment, we set pedestrians walking down a long narrow corridor 1.0 meters wide. The passageway was not wide enough to allow pedestrians to pass one another (Figure 4.3). We noticed that even when pedestrians are walking in a straight line, they still exhibit a natural side to side motion.

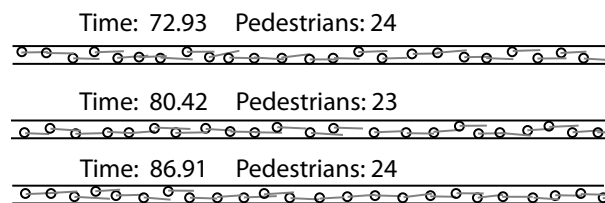


FIGURE 4.3. Snapshots from hallway experiments showing pedestrians walking down narrow corridor.

This secondary motion adds to the realism of the simulation as it is characteristic of actual human motion. When real people walk, they sway from side to side with each footfall. We also observed pedestrians trying to avoid walking directly behind other pedestrians and forming a zipper-like pattern.

In our final visualization experiment, we used our capability-behavior model to simulate an orderly evacuation of a large auditorium filled to 98% capacity and several adjacent offices (Figure 4.4).

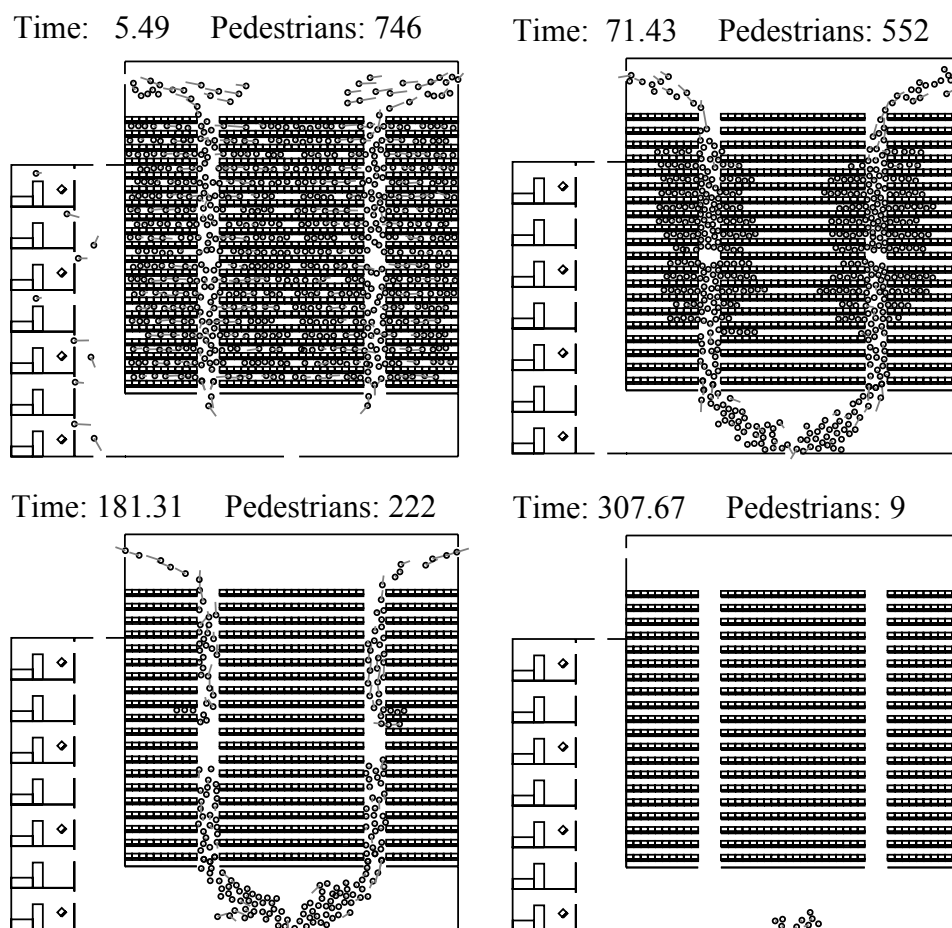


FIGURE 4.4. Snapshots from a simulation of 746 pedestrians evacuating an auditorium and adjacent offices. Total egress time for this simulation was 5 minutes and 16 seconds.

We simplified the simulation by assuming all the pedestrians have the goal of leaving the building through the nearest exit and all start egress at the same time. We know from social psychology and from accounts of actual evacuations that these are not accurate assumptions and, as such, can adversely affect the realism of the simulation [3, 19, 22]. In contrast, if we had added the ability to specify a start delay and had some pedestrians exit the way they came in, we could have added to the realism of the simulation. However, since the simulator is not the focus of the work, rather, the motion of the individual pedestrians, we feel justified in making those assumptions. Even using this simplified simulator, our large scale simulation experiment shows it is capable of moving pedestrians around in a more complicated setting.

## 4.2. Quantitative Analysis

If we expect to be able to use the simulation for evaluating the design of buildings for safe egress, we need to be confident that the motion is accurate. Qualitative analysis is not sufficient for determining the accuracy of our simulation. We need to be able to perform a quantitative analysis of our model. Validation of pedestrian simulations through quantitative measure poses an interesting challenge of data collection; it is one of the reasons why validation of pedestrian simulations is lacking [13]. Comparing our model against data from real evacuations is ideal. However, acquiring that data can be difficult. We do not have the right equipment set up in buildings to be able to record data during an emergency, and there is no guarantee that if we did, the equipment would work properly. For example, if we used video cameras to record an evacuation of a building, smoke from a fire may block its view, or flames may completely

disable it. Instead we rely heavily on data collected from personal accounts and 911 emergency calls to piece together evacuation behavior and response times [3]. Unfortunately, personal recollections can become distorted and may not yield the most accurate measure of event timing.

Since data collection during an actual emergency can be difficult, some researchers have begun to collect data to study pedestrian behavior in controlled environments [7, 26, 13]. Helbing *et al.* studied the flow of pedestrians through bottlenecks for uni- and bidirectional streams as well as the flow of two perpendicular intersecting streams [13]. They set up tables in different configurations to create the boundaries for the experiments. In each case, the pedestrians were told to walk through the setup and then return to the start to maintain a continuous stream of people. Daamen and Hoogendoorn performed similar experiments to observe the behavior of pedestrians in uni- and bidirectional streams under varying speed distributions, as well as the crossing of two and four pedestrian streams [7]. They have also studied the effect of widening bottlenecks on the flow of pedestrians. Seyfried *et al.* conducted experiments in controlled environments as well; their team focused their attention on single file movement and measuring the speed and density of pedestrians as they walked through a small data collection region [26].

Safe and controlled experiments cannot fully replicate the conditions of an actual emergency. Therefore, the accuracy of results obtained from these experiments is questionable. Thus a quantitative analysis is limited by a lack of real evacuation data available for comparison.

A method of validation commonly used is to compare the velocity, density, and flow of pedestrians through a space to the fundamental diagram (Figure 4.5). The fundamental diagram explores the relationship between these quantities. As

density starts to increase the flow of pedestrians will also increase, however, once the capacity of the space is reached, the flow will start to decrease. Likewise, the flow of pedestrians through a space is the same when there are fewer pedestrians traveling at higher velocities as when there are many pedestrians traveling at lower velocities. One can also compare the relationship between density and velocity. Generally, as the density grows the velocity of the pedestrians decreases. Daamen *et al.* has assembled the experimental findings of many researchers and illustrates the resulting fundamental diagrams as shown in figure 4.5 [8]. The results show similar trends, but the curves are not identical.

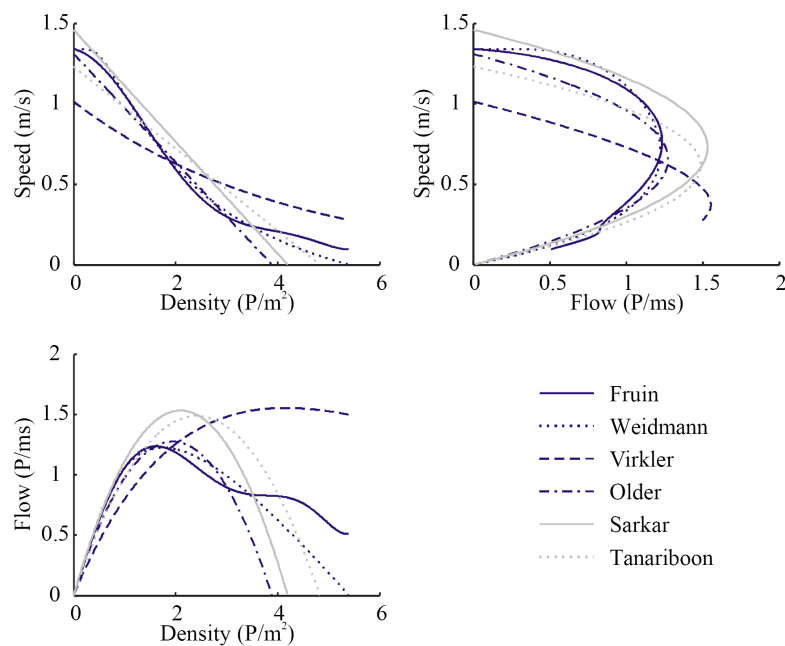


FIGURE 4.5. Fundamental diagrams showing the relationships between density and speed, flow and speed, and density and flow. Figure courtesy of Daamen *et al.*



Seyfried *et al.* have focused their attention on the relationship between velocity and density. They argue that the dependence between velocity and density is not completely understood and that the differences in the experimental findings of Figure 4.5 are rooted in the complexity of the problem [26]. They claim that passing maneuvers and other observed self-organization phenomena, such as lane formation and zipper effect, that are common for movement in a plane can influence the relationship between velocity and density. For example, by forming lanes pedestrians can maintain a higher velocity in greater densities than they would otherwise. To better understand the fundamental relationship, Seyfried *et al.* restrict the problem domain from movement in a plane to movement along a line, in an effort to simplify the problem and limit the effect of the influencing factors in a natural way. They conducted an experiment to collect velocity and density information as pedestrians walked in a single file line along an elliptical track. In an effort to validate our motion model, we tried to replicate the experiments and procedures described by Seyfried *et al.* and compare our results [26]. The rest of this section discusses our experimental setup, trials, and findings.

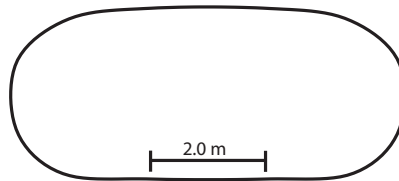


FIGURE 4.6. Experimental setup for the measurement of the velocity and density relationship for movement in a single file line.

We created an elliptical track measuring 17.3 meters in circumference. To measure velocity and density information we set up a data collection region 2.0 meters long in the middle of a straight portion of the track (Figure 4.6). The pedestrians walked clockwise following target locations along the track given by

the simulator. To try to prevent passing and enforce single file movement we simplified the cost function. We used only the distance and the deviation angle terms from the original cost function to rank movement options. The options that move the pedestrians closer and more aligned with the target were more likely to be chosen. We ran three experiments with  $N = 1, 15,$  and  $20$  pedestrians. To generate enough data we ran 5 simulations for 500 seconds for each experiment. To initialize the simulation we placed  $N$  pedestrians evenly spaced around the track. During the simulation, each time a pedestrian enters and leaves the data collection region the time is recorded. Afterward, we calculate the velocity for each pedestrian for each pass through the data collection region and calculate the average density during the time the pedestrian is inside this region. See table 4.1 for a summary of our results.

$N$	$\rho(1/m)$	$\rho^{Seyfried}(1/m)$	$\rho^{ours}(1/m)$	$v^{Seyfried}(m/s)$	$v^{ours}(m/s)$
1				1.24 (0.15)	1.23 (0.07)
15	0.87	0.77 (0.12)	1.29 (0.17)	0.90 (0.05)	0.86 (0.15)
20	1.16	1.07 (0.11)	1.50 (0.35)	0.56 (0.05)	0.68 (0.27)

TABLE 4.1. Comparison of mean and standard deviation from Seyfried *et al.* and our experiments. The first column shows the number of pedestrians on the track. The second column is the density measured over the entire length of the track. The third and fourth columns measure the density in the data collection region from Seyfried *et al.* and our experiments. The fifth and sixth columns report the velocity of the pedestrians as they pass through the data collection region.

Seyfried *et al.*'s results show little variance among the pedestrian's velocities, suggesting everyone all kept a steady speed. To get the average velocity for 1 person, Seyfried *et al.* considered the walking speeds of all 34 subjects as they

walked one at a time around the track [26]. The density variance also suggests the pedestrians maintained a fairly even spacing as they walked around the track. In our experiments, we witnessed the simulated pedestrians walking faster to fill the gap between them and the pedestrian in front but then slowing down again to try to avoid a collision. This behavior could explain the larger variance and difference in velocities. The speeding up and slowing down caused the pedestrians to bunch up, creating a shock wave that propagated around the track. This phenomenon could explain the higher densities recorded by our simulation.

To determine how close our model fits the velocity and density data collected from Seyfried *et al.*'s experiments we ran a hypothesis test. The formulation of our null hypothesis,  $H_0$ , and alternative hypothesis,  $H_a$ , is as follows:

$$H_0 : \mu_s = \mu_o$$

$$H_a : \mu_s \neq \mu_o$$

In other words,  $H_0 =$  the velocity/density of the pedestrians in Seyfried *et al.*'s experiment is the same as the velocity/density in our experiment, and  $H_a =$  the velocity/density of the pedestrians in Seyfried *et al.*'s experiment is different than velocity/density in our experiment.

To assess the validity of our null hypothesis at the 0.05 level of significance we ran a t-test [23]. We set the degrees of freedom to be  $df = 33, 14,$  and  $19$  for the respective case of  $N=1,15,$  and  $20$  pedestrians. In testing the velocity distributions, we found the t-value for the case of  $N=1,15,$  and  $20$  to be  $0.38,$   $2.99,$  and  $9.10$  respectively, and the p-value to be  $0.71,$   $0.0028,$  and  $2.3 \times 10^{-8}$  respectively. In testing the density distributions, we found the t-value for the case of  $N= 15$  and  $20$  to be  $16.64$  and  $16.17$  respectively, and the p-value to be

$7.8 \times 10^{-58}$  and  $1.5 \times 10^{-12}$  respectively. Generally, the smaller the p-value the greater the significance.

Therefore, there is significant difference in the mean velocities and densities in our experiment and Seyfried *et al.*'s experiment for  $N=15$  and  $20$  pedestrians. For the motion of 1 person, the evidence is not sufficient to show that the velocity of our simulated pedestrians is different from the velocity of the real people in Seyfried *et al.*'s experiment.

In our interest to validate our motion model for the individual pedestrians without the effect of passing maneuvers, self-organization behaviors, and environmental factors, we were lead to Seyfried *et al.*'s experimental setup and empirical findings. However, our efforts lead us to believe that the motion cannot be decoupled from the simulation, as the interactions between pedestrians and the environment affect how the pedestrian chooses to move. Unfortunately, this complicates a quantitative validation of our model, because any false assumptions or poorly modeled higher level behaviors affect the outcome. For example, in the single file line experiment, pedestrians have to negotiate how much space to leave between them and the person in front. If we modeled this poorly, it would be difficult to get an accurate picture of how well our motion model is performing.

## 5. DISCUSSION AND FUTURE WORK

Although our model produces motion that looks natural and crowd behavior that is plausible, in this chapter we discuss some of the problems we have with our approach and present some suggestions for future work.

### 5.1. Discussion

One of the strengths of our model is that it is built from motion capture data. This allows us to capture and create models from a wide range of individuals with different capabilities. This gives us the freedom to include many different pedestrian types in the simulation, such as able-bodied males and females of different ages, elderly individuals, people in wheelchairs and those using crutches, so that the composition of the crowds more accurately resembles reality. Rather than adjusting parameter values to include variation in crowds, we could draw from our database of models to create heterogeneous crowds more intuitively and accurately.

In addition, the motion of the individual pedestrians is more realistic. Since our capability-behavior model is based on the data we have collected, our simulated pedestrians can only make moves that are humanly possible. If pedestrians are walking quickly they will have to slow down before they can stop, whereas in other models they could stop unnaturally fast. Unfortunately, one of the strengths of our model is also one of its weaknesses. The simulated pedestrians' motions are limited to the type of data we have collected. If we had collected only clips of straight walking motions, that would be the only type of motion our simulated pedestrians could make. Similarly, if we did not collect enough slow walking motion, our pedestrians will not be able to walk slowly. To ensure that we have

provided for a range of locomotion types, for instance, fast walking, slow walking, and turning, we need to be sure we record an appropriate representative sample. When pedestrians are walking in high density regions they tend to walk very slowly at a pace that can be described as shuffling. We are using the motion collected from one subject who was not asked to provide samples of slow shuffling movements. At the time of collection, we did not recognize the importance of collecting very slow walking motions. This could explain the discrepancy in the velocities collected in our experiment of single file movement as well as the higher densities. Since there is not enough slow walking data the pedestrians are unable to choose these options. As a result they walk faster and may collide with the pedestrian in front. We stop the offending pedestrian by switching him to a standing pose; it takes a little while for him to recover his speed which causes the pedestrians behind him to slow. This creates a shock wave that propagates around the track and higher densities to be recorded in the data collection region. To solve this issue we need to be sure we capture all of the motion necessary for our pedestrians to perform the required tasks.

We have created a model for the motion of individual pedestrians, but in microscopic simulations the interactions between pedestrians must also be modeled. If we do not have a good sense, for example, of how and when people resolve collisions, how much space they prefer to have around them, or when they might decide to overtake the person walking in front, our simulation will not produce as accurate results. Unfortunately, these interactions can make it difficult to separate the testing of the motion model from the simulation.

In our experiments we observed pedestrian interactions that were less than realistic. For example, in our doorway experiment we noticed pedestrians near the back and on the sides overtaking other pedestrians to get close to the door.

This idea is realistic, but the execution of the action is not what we would expect from our experience. From our experience we know that people on the sides of congestion have more freedom to move faster and cut in front of a lot of the congestion. What seems unrealistic in our example is that the pedestrians start to move to the front, but then hesitate and wait behind other pedestrians instead of moving all the way to the door. When choosing movement options with our current cost function, the pedestrians must weigh the cost of taking a longer path to the exit but in a shorter amount of time against waiting behind other pedestrians to follow the shortest path out of the building.

At higher densities the space is more congested, and pedestrians must interact with each other and make more collision negotiation decisions. An effort was made to include this in our cost function so that pedestrians could consider their proximity to others when choosing a movement option. Ideally, the pedestrians would choose moves that keep them from colliding into other pedestrians. In practice, this was not always the case. Even the best laid plans can fail. Suppose our pedestrian chose an option that was predicted to keep it away from other pedestrians, but the other pedestrians took slightly different paths or changed speeds. It would be possible for our pedestrians to collide with each other. In addition, assigning a high cost to a mobility point may not guarantee that the pedestrian will not intersect the predicted position of another pedestrian. It will indeed be chosen if all other points cause a collision with static obstacles or walls. This is why we test at each step in the simulation for actual pedestrian collisions.

Perhaps our simple approach was not an adequate model for predicting how people make decisions about navigating around others. We need to have something in place to be able to run simulations with many people. However, a more accurate way to model collision avoidance and negotiation behavior might

be to abstract it out from the cost function and instead use a simplified model considering only distance and deviation angle from the target in the cost function and develop a better system for handling higher level behaviors.

To be able to isolate and validate only our motion model we could set up a Turing test. We could create two videos: one video showing a digitized version of a real person walking, and the other video showing a simulated pedestrian walking using our capability-behavior model. To create the video of a real person walking, we could record that person's motion from overhead and then digitize the video to create a 2D animation in the same style as our simulated pedestrian's video. We would ask subjects to watch each video and tell us which one they think is the real person and which one is simulated. If the subjects are unable to identify the simulated pedestrian, then we could say our model produces realistic and accurate motion.

Although each pedestrian is performing only local search over its list of capabilities, they are spending too much time calculating the cost of each of the movement options and searching through to find the best move that does not intersect with static objects in the scene. The average number of movement options in each cluster is approximately 1034 with a standard deviation of 467, compared to the average of 38 options in Srinivasan *et al.*'s approach [24]. With such a large number of movement options to search through, our approach slows considerably.

## 5.2. Future Work

Although we have demonstrated realistic motion of 2D pedestrians in several examples, there are areas within our approach that could be improved with



further effort and future work. To date, we have captured the motion from a single individual. Though we have demonstrated we can produce plausible crowd motion when each of those pedestrians are drawing from the same mobility map, we hypothesize that incorporating motion from individuals with varying abilities will enhance the realism of our simulations. We plan to collect additional motion capture data from a greater diversity of pedestrians. We would like to capture individuals with crutches, canes, in wheelchairs, and of varying ages (children and elderly), for both males and females. We would process their motion to build a more diverse database of 2D motion models. The clustering step would need to be modified to accommodate the differences in locomotion styles among a diverse population. For example, in determining the clustering for an able-bodied pedestrian we were able to ignore the joints in the upper body and compare the similarity of poses by examining the lower half of the body. These lower body joints, however, are probably the least important to a pedestrian using a wheelchair, and thus for determining the similarity between poses we would compare the upper body joints.

Our intention is to create models that can be used in large scale, real-time simulators. Before our model can meet this standard, we need to make it smaller and faster. Without rendering and detecting collisions, our simulator can update the positions of up to 140 pedestrians in real-time using an Intel Pentium 4, 3.2 GHz processor with 1.0 GB of RAM. This result is not as good as the approach by Srinivasan *et al.* [24], and not nearly good enough to provide the motion for large simulations in real-time. With our current approach we are unable to simulate large numbers of pedestrians in real-time. This is due in part to the time spent searching through the large numbers of movement options in each cluster and in part to the size of the mobility map. Although pedestrians of the same type, for

instance, all single able-bodied males between the ages of 30-35, can share a single mobility map in memory, one mobility map still requires 64 MB of storage space.

We are investigating ways to eliminate the need to search through and store movement options. To reduce storage, we could build the mobility map as described and then remove the pose from consideration. Our original mobility map had, from any pose state, a set of movement options that consisted of the positions it can reach in a small time frame, the final orientation, and the sequence of poses to get it there. In this case, we would treat the pedestrian's state as its velocity and orientation. From any state, the set of movement options from the mobility map would be the final positions and orientations, and all of the actual motion that was originally stored would be removed and replaced at run-time with a simple interpolation scheme. Pedestrians would interpolate their position and orientation over the time interval to get to the position and orientation specified by the mobility map. This approach would likely produce more realistic motion than using social forces alone, but not as realistic as the full pose approach that we are currently using. Removing the pose from consideration will reduce the amount of storage but at the expense of losing some of the important information associated with a pose. A pedestrian in one pose may have a similar velocity and orientation as another pose but have different dynamics. Also, this approach would not improve the time spent searching through the movement options.

Another method for reducing our storage requirements would be to examine the mobility map and remove the redundant options. Options that lead the pedestrian to similar positions with similar orientations are considered redundant. During the clustering process the mobility maps of similar poses were combined to yield a more complete set of options. However, since all of the poses in each cluster share similar dynamics the likelihood that some of the poses also share

similar positions and orientations is high. By removing these redundant options we hope to reduce the size of the mobility map without effecting the quality of the motion. Preliminary results have shown a reduction in the size of the unclustered mobility map by 85%.

The previous approaches still require us to store movement options and search through each one to find the best move; we would like to eliminate this need altogether. We have been looking at statistical versions of our current model in hopes of meeting this need. We are investigating replacing the movement options with movement option distributions that encode the capabilities of a pedestrian from a given pose with statistical measures.

Once our capability-behavior model is smaller and faster, and we have built a database of diverse models from a heterogeneous population, we would like to make our models available for others to use and incorporate into their own simulations. To improve realism, our model constrains the motion of simulated pedestrians to moves humans are capable of given a current state. It is not restricted to use within our own simulator. We are exploring ways of incorporating our motion model into existing simulation techniques, such as the social force model. We aim to improve the realism of the social force model by using our model to generate the motion of the 2D pedestrians. We propose the social force equations be used to rank the movement options instead of our cost function. The option with the lowest cost in terms of the social forces would be chosen as the pedestrian's next movement. There may be times when none of the movement options are able to meet the social force constraints, i.e., the cost to make the move exceeds a threshold. In these situations, we envision a hybrid approach where we use our motion model when possible and resort to the simple social force model when there is a problem.

Our present pedestrian simulation system uses some simplifying assumptions to include higher level behaviors, such as route choice and collision negotiation and avoidance. For example, it assumes pedestrians leave buildings through the nearest exit and pedestrians moving away from collisions go first. A better approach would be to use higher level behaviors as a way to direct the choice in movement options. We are investigating adding higher level behaviors, such as route-choice, grouping, collision negotiation and avoidance, that would sit on top of our motion model. The behaviors would be included in the cost function used to rank the movement options and will lead to a choice appropriate for that desired behavior. For example, a pedestrian walking with a group should pick different options than if it were trying to pass another pedestrian. To ensure the greatest accuracy in the design of the behaviors, they should be grounded in social psychology literature.

## 6. CONCLUSION

Realistic and accurate models of how people move are needed to evaluate the design of facilities for fast and efficient egress of large, diverse populations. These models should generate realistic motion for the individual pedestrians and should provide for the ability to simulate heterogeneous crowds. Furthermore, these models could be used in simulations for evacuation training and evaluating effective emergency response plans. We hypothesize that as we get closer to simulating real human motion, the simulations will become more accurate. This greater accuracy allow us to better identify weaknesses of existing measures and improve procedures and designs to help prevent human casualties.

Our model can automatically incorporate a pedestrian's physical limitations and capabilities when making movement decisions, since it takes into account the current configuration of the character. Our model leverages motion capture data to generate plausible motion. Although we have found significant evidence showing us that our model does not yet match speeds and densities for single file movement of 15 people and more, we are hopeful that with the inclusion of slower walking data and the addition of higher level collision avoidance and negotiation behaviors, we will see improvements in our accuracy.

We have shown that our model can reproduce some realistic crowd dynamics, such as jamming at doorways, and self-organization effects, such as the tendency of individuals walking in narrow spaces to form a zipper-like pattern. In addition, future models can also be built for generating heterogeneous crowds by collecting motion capture data that includes children, the elderly, pedestrians in wheelchairs, and people on crutches.

**BIBLIOGRAPHY**

- [1] G. Antonini, M. Bierlaire, and M. Weber. Simulation of Pedestrian Behavior using a Discrete Choice Model Calibrated on Actual Motion Data. In *4th Swiss Transport Research Conference*, Monte Verita, Ascona, Switzerland, 2004.
- [2] O. Arikan and D.A. Forsyth. Interactive Motion Generation from Examples. *ACM Transactions on Graphics*, vol. 21, pp.483-490, 2002.
- [3] J.D. Averill, D.S. Mileti, R.D. Peacock, E.D. Kuligowski, N. Groner, G. Proulx, P.A. Reneke, and H.E. Nelson. Occupant Behavior, Egress, and Emergency Communications. Federal Building and Fire Safety Investigation of the World Trade Center Disaster, NIST NCSTAR 1-7, 2005.
- [4] V.J. Blue and J.L. Adler. Emergent Fundamental Pedestrian Flows from Cellular Automata Microsimulation. *Transportation Research Record*, vol.1644, pp.29-36, 1998.
- [5] D.C. Brogan and J.K. Hodgins. Simulation Level of Detail for Multiagent Control. In *Proceedings of the First International Joint Conference on Autonomous Agents and Multiagent Systems*, pp.199-206. ACM Press, 2002.
- [6] W. Daamen. SimPed: A Pedestrian Simulation Tool for Large Pedestrian Areas. In *Conference Proceedings EuroSIW*, 2002.
- [7] W. Daamen and S.P. Hoogendoorn. Controlled Experiments to Derive Walking Behavior. In *European Journal of Transport Infrastructure Research*, vol.3(1), pp.39-59, 2003.
- [8] W. Daamen, S.P. Hoogendoorn, and P.H.L. Bovy. First-order Pedestrian Traffic Flow Theory. In *Transportation Research Board Annual Meeting*, pp.1-14, 2005.
- [9] I. Gargantini. An Effective Way to Represent Quadtrees. In *Communications of the ACM*, vol.25(12), pp.905-910, 1982.
- [10] D. Helbing. A Fluid Dynamic Model for the Movement of Pedestrians. In *Complex Systems*, 6: pp. 391-415, 1992.
- [11] D. Helbing and P. Molnar. Social Force Model for Pedestrian Dynamics. In *Physical Review*, vol.51, pp.4282-4286, 1995.
- [12] D. Helbing, I.J. Farkas, P. Molnar, and T. Vicsek. Simulation of Pedestrian Crowds in Normal and Evacuation Situations. In *Pedestrian and Evacuation Dynamics*, pp.21-58. Springer, Berlin, 2002.

- [13] D. Helbing, L. Buzna, A. Johansson, and T. Werner. Self-organized Pedestrian Crowd Dynamics: Experiments, Simulations, and Design Solutions. In *Transportation Science*, vol.39(1), pp.1-24, 2005.
- [14] L. Henderson. The Statistics of Crowd Fluids. *Nature*, 229: pp.381-383, 1971.
- [15] S.P. Hoogendoorn and P.H.L. Bovy. Gas-Kinetic Modeling and Simulation of Pedestrian Flows. In *Transportation Research Record*, 1710: pp. 28-36, 2000.
- [16] R.L. Hughes. A Continuum Theory for the Flow of Pedestrians. In *Transportation Research Part B*, 36: pp.507-535, 2002.
- [17] T. Kim, S.I. Park, and S.Y. Shin. Rhythmic-Motion Synthesis Based on Motion-Beat Analysis. In *ACM Transactions on Graphics*, vol. 22, pp.392-401, 2003.
- [18] L. Kovar, M. Gleicher, and F. Pighin. Motion Graphs. In *ACM Transactions on Graphics*, vol.21, pp.473-482, 2002.
- [19] B. Latane and J.M. Darley. Group Inhibition of Bystander Intervention in Emergencies. In *Journal of Personality and Social Psychology*, vol.10, pp.215-221, 1968.
- [20] J. Lee, J. Chai, P.S.A. Reitsma, J.K. Hodgins, and N.S. Pollard. Interactive Control of Avatars Animated with Human Motion Data. In *ACM Transactions on Graphics*, vol.21, pp.491-500, 2002.
- [21] R. Metoyer. Building Behaviors with Examples, Ph.D. Thesis, 2002.
- [22] G. Proulx. Occupant Behavior and Evacuation. In *Proceedings of the 9th International Fire Protection Symposium*, Munich, pp. 219-232, 2001.
- [23] F.L. Ramsey and D.W. Schafer. *The Statistical Sleuth: A Course in Methods of Data Analysis*, 2<sup>nd</sup> Ed., Belmont, CA: Duxbury Press, 2002.
- [24] M. Srinivasan, R.A. Metoyer, and E. Mortensen. Controllable Real-Time Locomotion using Mobility Maps. In *Proceedings of Graphics Interface*, Victoria, B.C., pp. 51-59, 2005.
- [25] M. Srinivasan and R. Metoyer. A Responsiveness Metric for Controllable Characters. *Technical Report #CS05-50-01*, School of Electrical Engineering and Computer Science, Oregon State University, 2005.
- [26] A. Seyfried, B. Steffen, W. Klingsch and M. Boltes. The Fundamental Diagram of Pedestrian Movement Revisited. In *Journal of Statistical Mechanics: Theory and Experiment*, P10002, 2005.

- [27] Vicon, Vicon 612 optical motion capture system, <http://www.vicon.com>, 2004.



